Sensitivity analysis of collisional processes in a detached plasma in Magnum-PSI with B2.5-Eunomia

R. Chandra, H. J. de Blank, P. Diomede, E. Westerhof

DIFFER - Dutch Institute for Fundamental Energy Research, Eindhoven, The Netherlands

Introduction

The realization of fusion energy requires breakthroughs in divertor control to withstand the tremendous heat flux from a burning plasma. One solution is to operate in the detached plasma state. Reaching and controlling this state require better understanding of the underlying mechanisms. By using linear plasma generators, the repetitive rate of discharges is very high, diagnostics are more flexible and with superconducting coils steady-state plasmas are achievable. With the addition of computational modelling, atomic processes can be investigated using data from experiments and then be transferred to more sophisticated tokamak models. In this paper we present our analysis of the detached plasma experiments in Magnum-PSI [1], where it was achieved by increasing the neutral background pressure or injecting impurities in the target vicinity, decreasing energy and particle fluxes to the target [2, 3]. We study the relevance of collisional processes to reach the detached plasma state.

B2.5-Eunomia: Modelling constraints

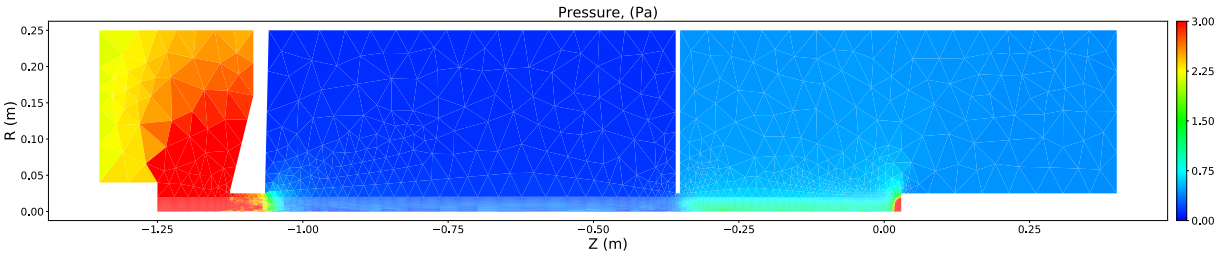

Figure 1: *Simulation domain with different neutral pressures mimicking Magnum-PSI conditions. The plasma source is located at* $Z = -1.25$ *m and the target is at* $Z = 0.029$ *m. Pressures for each chamber are controlled to be, from the plasma source, 1.956 Pa, 0.412 Pa, and 0.45 Pa respectively.*

We use B2.5-Eunomia [4] to model Magnum-PSI experiments on detachment of hydrogen plasma (#13941-13944, #13946, and #13948). In these experiments the neutrals pressure in the source chamber and the target chamber was kept at 1.956 and 0.412 Pa respectively. We use electron density and temperature radial profiles measured from Thomson scattering (TS) as our plasma source boundary condition. The plasma source has parameters: $n_{e,\mathrm{peak}} = 2.667 \times 10^{20}$ m^{-3}, $T_{e,\mathrm{peak}} = 2.47$ eV, and Gaussian FWHM $= 1.589$ cm. Additionally, we impose zero gradient for the velocities, and a potential profile is given with an old profile from plasma

rotation measurement [5] that is adjusted to give better convergence. For the target we impose the velocity to be equal to sound speed and the potential is floating. The plasma recombines at the target providing neutral flux, 90% H and 10% H_2, based on the incoming ion flux. We prescribe constant diffusion coefficients for plasma cross-field transport based on the average collision time. We then recreate the experiment by varying the pressure at the target chamber with values 0.45, 0.9, 1.4, 2.0, 3.1, and 4.0 Pa while keeping all other boundary constraints unchanged.

Particle flux

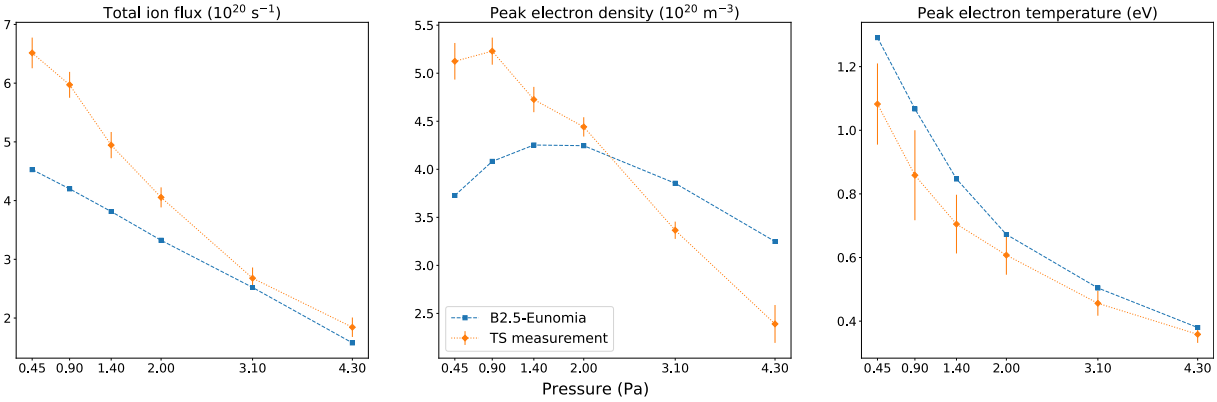

Figure 2: *Comparison of ion flux, peak electron density, and peak electron temperature at $Z = 0.0$ m between modelling and experiments. B2.5-Eunomia is able to reproduce the ion flux reduction with increasing neutral pressure. Electron temperature evolution is in good agreement with TS measurements. Electron density calculated from the model does not follow the experimental trend.*

In Figure 2 we show the ion flux, peak electron density and peak electron temperature from B2.5-Eunomia results and TS measurements at $Z = 0.0$ m. The TS ion flux is calculated using the formula $\Gamma = \frac{1}{2} n_{e,TS} \sqrt{\frac{2T_{e,TS}}{m_p}}$ and integrated over the radius. We see that B2.5-Eunomia is capable of reproducing the reduction of proton flux with increasing pressure. The model is also able to produce similar electron temperatures. We observe a discrepancy in the peak electron density, where the model fails to reproduce the downward trend with increasing neutral pressure. We suspect there might be collisional processes that enhance recombination that are not present in the model.

Relative contributions of collision processes in ion and momentum losses

The reduction of ion flux is caused by ion particle and momentum losses. These losses can be attributed to transport or volume processes. In our model we observe that plasma radial flow is negligible compared to parallel flow, so most loss contribution is coming from volume processes i.e. electron-ion recombination, molecular-assisted recombination (MAR) with H_2^+ and mutual recombination with H^-. In Figure 3a we show the contributions of each particle loss process for

different pressures. The contributions are described by the collision frequency of each process. Here we observe that two and three-body recombination is the major contributor for every pressure case. We can also observe a sudden rise in the production of H_2^+, which is the MAR process. This is caused by H_2 gas puffing to achieve neutral pressures of 1.4 Pa and higher. The recombination path via H^- does not contribute much on the overall particle loss rate. In the case of momentum loss, elastic ion-neutral collisions are the dominant processes, shown in Figure 3b. Elastic scattering of ions with atomic hydrogen is shown to be the dominant process. We observe that elastic p-H_2 collision is radically enhanced via gas puffing and increases with higher neutral pressure.

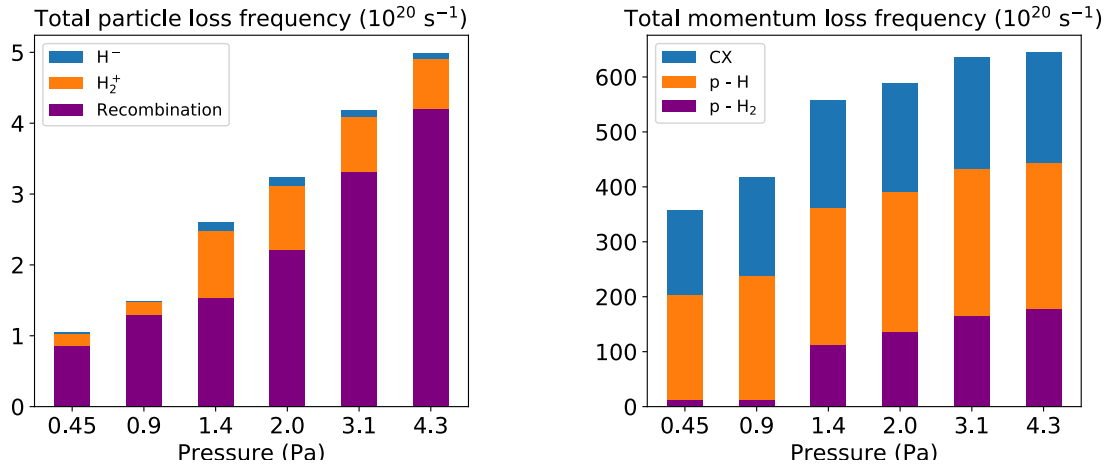

(a) (b)

Figure 3: *(a) Total H^+ particle loss frequency in the plasma beam. The blue and orange color represent the gross production of H^- and H_2^+ which lead to H^+ recombination. The purple color represents two and three-body recombination rate. (b) Total H^+ momentum loss frequency. Blue represents charge exchange events, orange represents elastic scattering with atomic hydrogen, and purple represents elastic scattering with hydrogen molecules.*

Gas puffing increases the density of H_2, thereby increasing the rate of MAR. We can observe this by calculating collision frequencies locally in the simulation. In Figure 4 the collision frequency of MAR is shown. It is clear that MAR events are significantly higher at pressure 1.4 Pa and above. In the same figure the electron-ion recombination frequency is also highlighted. We discover that significant frequency locations do not overlap between MAR and electron-ion recombination. Looking back to Figure 3a we observe that the total MAR events after puffing do not increase, however the vice versa applies to electron-ion recombination. Therefore, we conclude that MAR acts as an additional process for particle loss and enhances electron-ion recombination at large neutral densities.

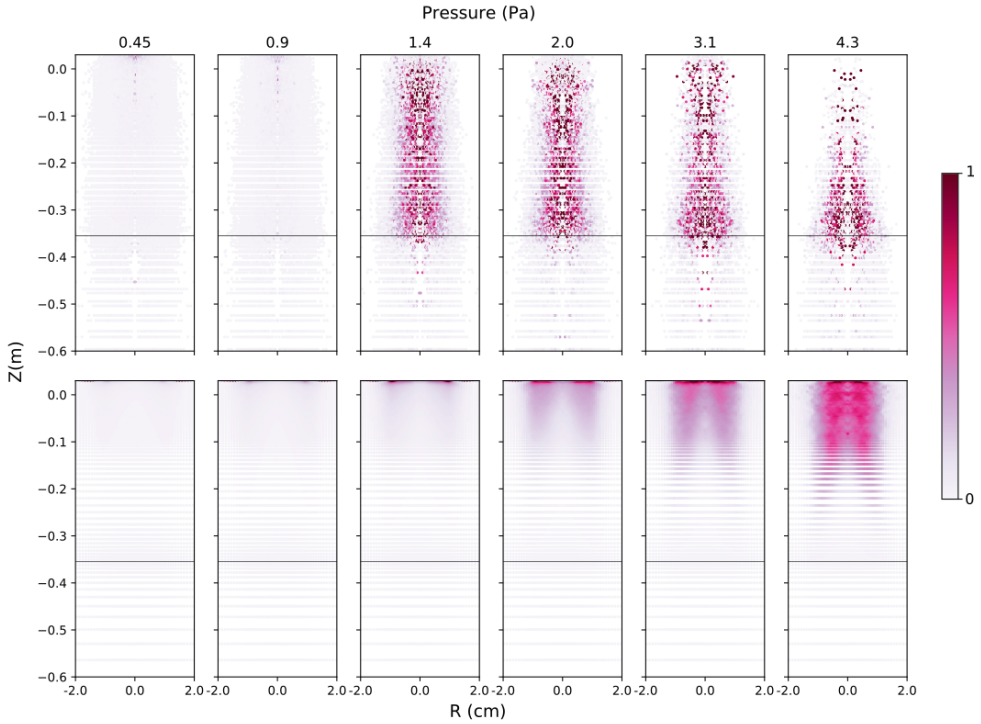

Figure 4: *Location of MAR (top) and electron-ion recombination (bottom) events. The domain is limited to $Z > -0.6$ m since most of the events occurs at this location. The black line indicates the location of the skimmer. The colors indicate the collision frequency normalized to volume and maximum values of each process. The MAR process becomes significant at pressures above 1.4 Pa, while electron-ion recombination is increasing with higher pressure settings.*

Importance of H_3^+

The discrepancy between the density profile obtained from B2.5-Eunomia and experiments indicates that additional recombination processes are necessary. Cross-sectional data [6] suggest that collision of H_2^+ with H_2 producing H_3^+ is competitive with the implemented $e-H_2^+$ recombination at energies below 8 eV. The latter reaction are not fully recombinational i.e. the resulting H^* atom can re-ionize into a proton, which can have significant fraction in the recorded collision frequencies for MAR shown in Figure 3a. Recombination through H_3^+ still requires prior production of H_2^+ through MAR, hence its importance can be inferred once the n_e and T_e dependent ratio between reionization and de-excitation of H^* atom at MAR locations is established.

References

[1] G. de Temmerman, et al., Fusion Eng. Des. 88:6-8, 483 (2013)

[2] R. Perillo, et al. Nuclear Materials and Energy 19:87-93 (2019)

[3] K. Jesko, PhD thesis, TU/e and Aix-Marseille University (2018)

[4] R. C. Wieggers, et al., Contrib. Plasma Phys. 52, 440 (2012)

[5] R. C. Wieggers, et al.,J. Nuc. Mat. 438, S643-S646 (2013)

[6] T. Tabata, et al., At. Data Nucl. Data Tables 76, 1:1-25 (2000)